

Surface segregation of third-column atoms in group III-V arsenide compounds: Ternary alloys and heterostructures

J. M. Moison, C. Guille, F. Houzay, F. Barthe, and M. Van Rompay

Laboratoire de Bagneux, Centre National d'Études des Télécommunications, 196 avenue Henri Ravera, F-92220 Bagneux, France

(Received 9 January 1989)

We report a systematic study of the segregation of third-column elements involved in group III-V arsenide structures to their (100) surface. The surface composition is obtained by *in situ* electron spectroscopies, on special structures built by molecular-beam epitaxy. In ternary alloys, an important surface enrichment in one of the third-column components is most often observed, leading to a near-binary surface. Heterojunctions between two given binary materials *A* and *B* are abrupt or not in composition, depending on the growth sequence (*A* grown on *B* or *B* grown on *A*): for one sequence, the top monolayer of the base material is gradually distributed in the growing overlayer. All these behaviors can be summarized by tendencies to surface segregation following $\text{In} > \text{Ga} \geq \text{Al}$, and by segregation efficiencies that are either near zero or near unity depending on the way structures are built. The application of standard models to the segregation isotherms for ternary alloys yields segregation energies of 0.1–0.2 eV. The physical origin for the segregation process and its consequences on interface roughness along the growth axis are discussed.

I. INTRODUCTION

A fair part of the major recent achievements in semiconductor physics is based on the progress of growth techniques, and especially of molecular-beam epitaxy (MBE).¹ High-quality materials can now be built into complex tailored structures, such as quantum wells, superlattices, or graded heterojunctions. The quality of the structures themselves is illustrated in GaAs/Ga_xAl_{1-x}As superlattices where barrier-well interfaces are atomically flat over distances up to 1000 Å and accuracies on the well width of one atomic layer have been claimed.² The present challenges concern atom-sized structures, such as superlattice alloys, ultrathin quantum wells built with lattice-mismatched compounds, or fractional monolayer growth.^{3,4} Since pattern sizes are here atomic ones, the geometry must be controlled down to the submonolayer level, despite the enormously steep composition and lattice parameter gradients. Precautions must obviously be taken, such as minimizing the heterointerface roughness by growth interruptions⁵ or avoiding the switch from layer-after-layer growth to island growth for lattice-mismatched heterojunctions. However, unwanted atomic displacements may still limit the interface abruptness. At usual growth temperatures ($\leq 600^\circ\text{C}$), bulk diffusion is not operative due to the lack of vacancies;⁶ atomic arrangements are determined during growth by surface or near-surface processes and frozen after burial. On the other hand, the displacement of atoms at the growth surface only requires the temporary breaking of a limited number of bonds. These motions yield the high surface mobility which helps in eliminating growth defects, but they may also lead to exchanges between substrate atoms and impinging atoms due to preferential segregation to the surface of substrate atoms. This would result in

smoothing or even ruining the planned composition gradients.

Many examples of such phenomena have been known for a long time in metallurgical science:⁷ impurities segregate at surfaces or grain boundaries (e.g., carbon or sulfur in iron), and the surface composition of alloys is most often different from their bulk one (e.g., the surface of Fe-Cr alloys is Cr-rich). Similar alloy effects have been reported in III-V ternary alloys, where they involve only bulk-surface redistribution in one of the third-column or fifth-column atom sublattices. The surface composition of the ternary arsenide Ga_{0.7}Al_{0.3}As is found to be Ga-rich^{8,9} and those of Ga_{≈0.5}In_{≈0.5}As and Al_{≈0.5}In_{≈0.5}As alloys to be In-rich⁹ (surface segregation in the third-column atom sublattice within a common As sublattice). Surface segregation is also observed at heterointerfaces. We have shown that during the deposition of GaAs on InAs In-Ga exchanges drive In atoms on top of the growing GaAs overlayer.¹⁰ Similar results have been reported for the growth of AlAs on GaAs (Ga segregation)¹¹ and GaSb on AlSb (Al segregation).¹² For other semiconductor structures, during the growth of Si (Ref. 13) or Ge (Ref. 14) on GaAs, of Si on GaP,¹⁵ and of Ge on CuBr,¹⁶ both substrate constituent atoms segregate on top of the growing overlayer. Still more complicated cases are those of ZnSe on GaAs (exchange Se-As),¹⁷ or CdTe on InSb (exchange Te-Sb).¹⁸ Surface segregation may also prevent dopant atoms from getting correctly incorporated during the growth, or redistribute impurities like carbon.¹

Segregation theory has been established a long time ago in metallic alloys on a firm experimental basis, because many elements can be tested for segregation in a given matrix due to the flexibility of metals, because near-equilibrium thermodynamic conditions can be easily

attained, and also because the practical impact of segregation at grain boundaries on metal strength has been recognized very early. On the other hand, test structures built with semiconductors may be better defined and controlled than those built with metals, but only sparse and qualitative data have been reported for segregation in these systems, which are less varied and until now less critical, and which cannot be brought as near to the thermodynamical equilibrium as the metallic systems. We report here a first systematic and quantitative study of the segregation of third-column atoms at the (001) surface of the most commonly used ternary alloys ($\text{Ga}_{1-x}\text{Al}_x\text{As}$, $\text{Al}_{1-x}\text{In}_x\text{As}$, $\text{Ga}_{1-x}\text{In}_x\text{As}$) and at the corresponding (001) heterointerfaces (GaAs, AlAs, and InAs with each other) by *in situ* surface-sensitive techniques. We then discuss the possibility of applying standard segregation theory to these systems, essentially to the ternary compounds which are in a stationary state and not too far away from the genuine thermodynamical equilibrium. We finally evaluate the consequences of segregation phenomena on heterostructure geometry and properties.

II. BUILD-UP OF THE TEST STRUCTURES

For ternary alloys, we have grown by MBE thick (i.e., $>2000 \text{ \AA}$) layers of the desired material $A_xB_{1-x}\text{As}$ ($A, B = \text{In, Ga, or Al}$). The base substrate is GaAs in most cases, except for $\text{In}_{0.53}\text{Ga}_{0.47}\text{As}$ and $\text{In}_{0.52}\text{Al}_{0.48}\text{As}$, which have been grown on InP which is lattice-matched to them. When the lattice mismatch between layer and substrate is large ($\text{In}_{0.2}\text{Ga}_{0.8}\text{As}$ on GaAs, for instance), the first stages of the growth are perturbed [strained growth and/or three-dimensional (3D) growth], and the growth is prolonged until most of the ternary layer is strain-free, the lattice mismatch being undertaken by interface dislocations. For heterointerfaces, three types of structures have been used to decide whether B atoms segregate to the surface when a layer of an A -As material is grown on a buffer layer of a B -As one (see Fig. 1). First, since segregation occurs at the very first steps of

the interface build-up, we have investigated single atomic layers of an A -As material deposited onto a buffer layer of a B -As material, and checked by surface-sensitive techniques whether the expected geometry is actually obtained (type-I structure). For lattice-matched heterostructures, thin ($\leq 100 \text{ \AA}$) overlayers of the A -As material have been grown on a B -As buffer layer, and their surface analyzed in search of B atoms (type-II structure). For the same purpose in the case of lattice-mismatched materials, sandwich type-III structures—a buffer layer of B -As, a single atomic layer of A -As, and a thin ($< 200 \text{ \AA}$) overlayer of B -As—have been used in order to avoid the switch from 2D laminar growth to 3D island growth, and hence to keep the system as homogeneous as possible in the growth plane. The single atomic layer thickness unit (1 monolayer = 1 ML) is defined as one third-column plus one As buffer-layer-like (001) plane and is calibrated by reflection high-energy electron-diffraction (RHEED) oscillations during homoepitaxy,¹ with an accuracy estimated to be $\pm 5\%$.

MBE growth is performed under monitoring by 10-keV RHEED inside a Riber 2300 chamber connected to an analysis chamber with Vacuum Generators CLAM100 facilities for Auger electron spectroscopy (AES), x-ray photoemission spectroscopy (XPS), uv photoemission spectroscopy (UPS), and electron-energy-loss spectroscopy (EELS). Substrates and growth conditions are optimized for each structure or material desired, but some common classical rules are used. Single atomic layers are built at a growth rate of $\approx 0.5 \text{ ML/s}$, thicker layers ($50\text{--}500 \text{ \AA}$) at $\approx 0.3 \text{ ML/s}$, and buffer layers at $\approx 1 \text{ ML/s}$. The growth temperature is 600°C , except for In-containing layers where it is reduced to 480°C in order to avoid In desorption.¹⁹ Arsenic pressures are tuned in the $10^{-6}\text{--}10^{-5}$ -Torr range to the minimum pressure ensuring the "As-stabilized" regime except for In-containing layers, where the maximum pressure ensuring "In-stabilized" growth is used.¹⁹ The final thickness of the buffer layers is large enough to avoid effects of the initial contamination and to accommodate the eventual lattice

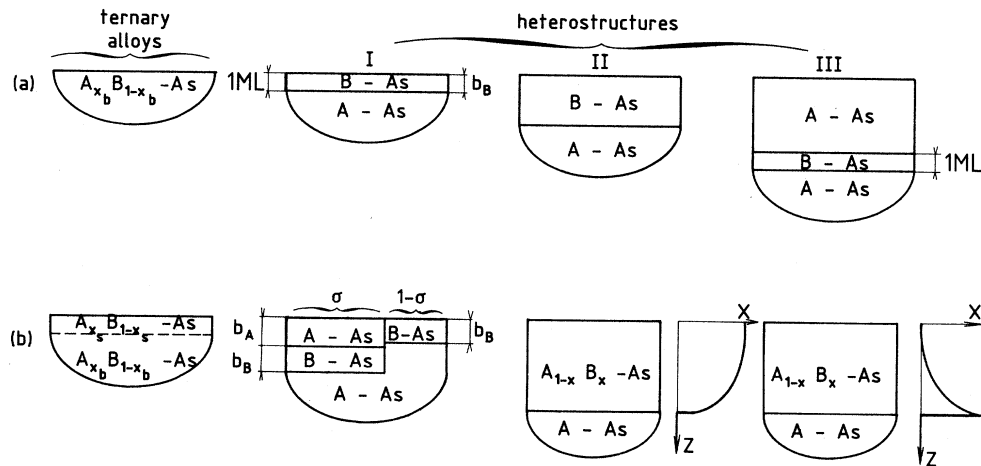


FIG. 1. Schematics of samples used, ternary alloys and heterostructures. For each kind of sample, (a) represents the planned geometry, and (b) the model used to interpret the AES-XPS data. For the models of type-II and type-III heterostructures, the concentration gradient is also indicated.

mismatch with the substrate, thus yielding clean and unstrained top layers. At each heterointerface, the growth is interrupted during about one minute in order to smoothen the surface,⁴ which is evidenced by an overall improvement of the RHEED pattern. Except during the initial stages of the buffer-layer build-up, RHEED patterns display short streaks, indicating planar layer-after-layer deposition. The integer-order streak spacing corresponds to the lattice parameter of buffer layers, with an accuracy of $\pm 3\%$, which grossly indicates that the type-III structures take the in-plane parameter of the substrate (pseudomorphism). The surface reconstructions are typical of (100) surfaces of III-V compounds and are discussed elsewhere.²⁰

III. SURFACE AND SUBSURFACE QUANTITATIVE ANALYSIS

After cooling down, first under As pressure down to 300°C and then under vacuum down to room temperature, samples were transferred under ultrahigh vacuum to the analysis chamber. Some samples have been analyzed *ex situ* by Rutherford backscattering (RBS) with 1-MeV He⁺ ions, but most measurements were done *in situ* by our surface techniques. The AES spectrum is taken with a normal-incidence 2-keV primary beam and a modulation of 2.5 eV peak to peak, the XPS spectrum with the natural Al *K*α line (1486.6 eV), the UPS spectrum with the He II line (40.8 eV), and the second-derivative EELS spectrum with a primary electron energy of 120 eV and a modulation of 1 eV peak to peak. All spectra are compared to those obtained under similar experimental conditions on GaAs, AlAs, and InAs buffer layers which will be referred to as standards. The energy positions of the AES and XPS peaks for structures and standards are not significantly different and only their intensity (peak-to-peak height for AES and peak area for XPS) will be discussed. The information provided on the electronic band structure by small UPS and EELS peak shifts is discussed elsewhere.²⁰ In EELS spectra, due to the derivation procedure, peak intensities are not fully reliable and only the absence or existence of peaks related to surface third-column atoms (e.g., transitions from core levels to surface states) will be taken into account here.

For XPS, AES, and to some extent UPS, a quantitative evaluation of the peak intensities may be performed. We first assume that the primary excitation (high-energy electrons, soft x rays, and uv light) is uniform since its absorption depth is large with respect to the escape depth of emitted electrons. Secondly, since all structures are formed by stoichiometric group-III-As compounds, their As bulk content is the same. Arsenic peak intensities corresponding to high electron energies and hence to high electron escape depths and low sensitivities to the surface should then be the same for all materials and structures. We shall use them as references in order to eliminate fluctuations in experimental conditions. It must be noted that surface-sensitive arsenic peaks may depend on group-III/As surface stoichiometry and then eventually on experimental conditions. For instance, a 30% variation of As coverage is estimated between the

most commonly obtained surface structures of GaAs, the $c(4\times 4)$ and (2×4) reconstructions.¹ This could create a $\approx 15\%$ uncertainty on the most surface-sensitive AES peaks, and a much smaller one ($\approx 5\%$) on XPS data. In order to obviate this problem to a certain extent, we take care to follow the same cooling-down procedure described above for standards and structures. In most cases, this yields the same surface reconstructions for both of them—for instance, $c(4\times 4)$ for GaAs, Ga_xAl_{1-x}As ternary alloys and GaAs/AlAs heterostructures—and presumably similar As surface coverages. Each signal originating from third-column atoms is then referred to the As signal from the same technique; for XPS where several As peaks are available, the reference will be the As peak having the highest kinetic energy (highest electron escape depth) and hence being the least sensitive to the surface. Finally, these peak ratios are in turn referred to their value in the corresponding standards. An example of the definition of this reduced ratio *R* for In by the XPS technique is given below:

$$R_{\text{In,XPS}} = \frac{[\text{In}_{\text{XPS}}]/[\text{As}_{\text{XPS}}]_{\text{in structure}}}{[\text{In}_{\text{XPS}}]/[\text{As}_{\text{XPS}}]_{\text{in InAs}}} \quad (1)$$

The final accuracy obtained on *R* for a given sample lies in the $\pm 15\%$ range for AES and in the $\pm 10\%$ range for XPS; sample-to-sample deviations will be reported with the data. A similar procedure is used for UPS, except that peaks (In 4*d* and Ga 3*d* core levels) are not referred to As peaks which cannot be detected with our UPS setup.

The reduced ratios depend only on the distribution of third-column atoms and also on the electron escape process. This process is taken into account by assuming that outgoing electron beams are attenuated following an exponential law with an escape depth *L* depending on their kinetic energy *E_k* in the crystal, but not on the material they pass through. *L*(*E_k*) is taken to be constant (5 Å) for *E_k* < 100 eV and proportional to the square root of the energy [*L*(Å) $\approx 0.5\sqrt{E_k(\text{eV})}$] above 100 eV, which roughly describes the experimental data.²¹ No correction for electron backscattering processes is made. All above assumptions are classical and are confirmed by the results we obtain on systems without segregation (see Ref. 22 and Sec. IV). Finally, we compare the experimental reduced ratios to expectations obtained from various models of the surface and subsurface where composition gradients are assumed to lie only in the growth direction (planar interfaces).

IV. RESULTS

A. Ternary alloys

For ternary alloys A_xB_{1-x}As, we consider thick (> 1000 Å) layers, which have presumably—this point will be discussed further on—their stationary composition gradient. The bulk composition *x_b* was checked by luminescence and also by the bulk-sensitive XPS peaks to be the one expected from the ratio of third-column-atom

fluxes. Since no third-column-atom redistribution can take place in the bulk, the composition gradient can exist only very close to the surface, where the atom mobility normal to the surface is high enough; the concentration gradient which cannot extend in the bulk is hence probably only limited by the surface roughness which lies in the ML range after growth completion. As a first-order approximation, we shall then assume that only the top surface monolayer has a composition x_s different from x_b . The reduced ratio R associated to element A is then

$$\begin{aligned} R_A &= \int_0^\infty x(z) e^{-z/L_A} dz / \int_0^\infty e^{-z/L_A} dz \\ &= x_s (1 - e^{-b/L_A}) + x_b e^{-b/L_A} \\ &= x_b + (x_s - x_b) (1 - e^{-b/L_A}) \\ &= x_b + (x_s - x_b) (1 - \epsilon_A), \end{aligned} \quad (2)$$

where z is the depth measured from the surface, where b is the separation between the topmost and second layers of third-column atoms, for which we shall substitute here half the lattice constant corrected by elastic deformations,²³ and where ϵ_A is $\exp(-b/L_A)$. For the most surface-sensitive peaks ($L=5 \text{ \AA}$), $\epsilon \approx 0.5$, and approximately half the signal comes from the top layer and the other half from the rest of the crystal, which gives us sufficient sensitivity to x_s variations. For more bulk-sensitive peaks ($L=20 \text{ \AA}$), ϵ and hence the sensitivity to x_s variations is lower but data accuracy is usually higher. Comparison between x_s values obtained for various probed depths indicates that our assumption that all the segregation is concentrated in the first layer is correct as a first-basis approximation. Surface-sensitive AES spectra (Fig. 2) show clearly surface enrichments. The values of x_s deduced from experimental R data by Eq. (2) for common ternary alloys are listed in Table I and mean values are summarized in Table II. More systematic x_s (x_b) measurements will be presented in Sec. V B. In spite of the rather high uncertainty on the x_s values, it is clear that the stationary surface composition of ternary alloys is not similar to their bulk one, and that the surface monolayer is actually purely binary. The fact that x_s values lie systematically above unity for $\text{Ga}_x\text{Al}_{1-x}\text{As}$ even suggests an enrichment of subsurface atomic layers. The surface enrichment is confirmed by EELS spectra (Fig. 3) which preferentially display transitions between core levels and surface states corresponding to surface-located segregated atoms. These results are in agreement with the XPS data of Stall *et al.*,⁸ which indicate that $\text{Ga}_{0.7}\text{Al}_{0.3}\text{As}$ has a GaAs surface. The tendency of third-column atoms to surface segregation, which can be summarized by the relation $\text{In} > \text{Ga} > \text{Al}$, is also in agreement with the results of Massies *et al.*;⁹ the quantitative differences between their results and ours—they find a systematically smaller enrichment—are due to different definitions of the “surface thickness.” Incidentally, it may be noted that annealing In-containing alloys at temperatures where In but not the other metal desorbs changes their surface composition to In-poor as expected.

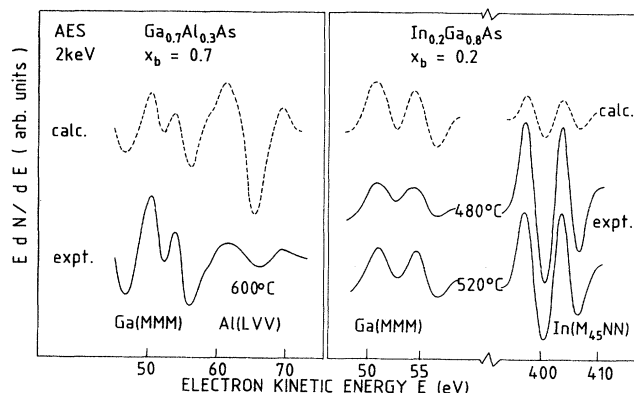


FIG. 2. AES spectra (solid lines) of (a) $\text{Ga}_{0.7}\text{Al}_{0.3}\text{As}$ and (b) $\text{In}_{0.2}\text{Ga}_{0.8}\text{As}$. For the second alloy, data corresponding to as-grown samples and postannealed samples are shown; the temperature indicated is the final one, i.e., respectively the growth temperature and the anneal temperature. The top spectra (dotted lines) are those which would be expected for no segregation. They are constructed by scaling each peak from the corresponding substrate by its fraction in the alloy, after reduction to the same As peak. For instance, the dotted spectrum of $\text{Ga}_{0.7}\text{Al}_{0.3}\text{As}$ is built with the Ga peak of GaAs scaled by 0.7 and the Al peak of AlAs scaled by 0.3; after that all three AES spectra have been normalized to have the same As peak. The values of x_s deduced from the comparison between experimental bottom spectra and theoretical top ones are listed in Table I.

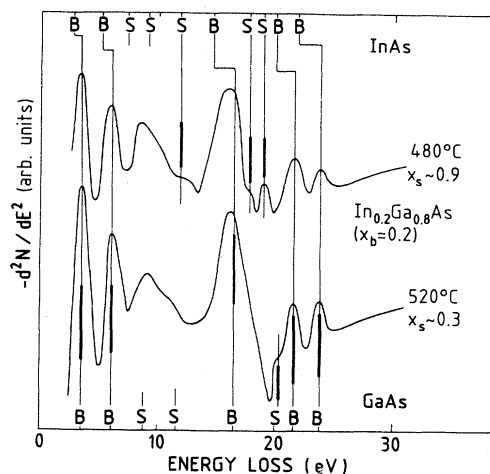


FIG. 3. EELS spectra of $\text{In}_{0.2}\text{Ga}_{0.8}\text{As}$, as-grown at 480°C , and after annealing at 520°C ; on each spectrum the indium surface content x_s deduced from AES-XPS measurements is indicated. Characteristic features of GaAs and InAs are drawn on the bottom and top scales as “GaAs” and “InAs,” and labeled S for peaks associated with transitions involving surface states and B for peaks involving only bulk states. While the bulk features are essentially stationary and similar to those of GaAs, as expected from the Ga-rich bulk composition, surface features turn from those of InAs to those of GaAs after annealing. Note particularly the doublet around 20 eV which is typical of In-related surface states and is replaced by the peak typical of Ga-related surface states (Ref. 20).

TABLE I. Bulk (x_b) and surface (x_s) compositions of selected III-V $A_xB_{1-x}As$ ternary alloys. In-containing alloys are either as-grown, or annealed at $> 500^\circ\text{C}$ under As pressure after the end of the growth in order to desorb the surface indium. For each case, the peak kinetic energies E_k , corresponding electron escape depths L , and reduced ratios R averaged on about five samples are listed. Surface-sensitive As peak to bulk-sensitive As peak ratios are referred to their values in the bulk binary material whose composition is the nearest from the deduced surface composition (for instance, InAs for the In-rich surface of $Ga_xIn_{1-x}As$ materials).

Alloy	Peak	E_k (eV)	L (Å)	R	x_b	x_s
$Ga_xAl_{1-x}As$ grown at 600°C	Al AES	66	5.0	0.06 ± 0.02	0.7	1.0 ± 0.3
	Ga AES	55	5.0	1.02 ± 0.20	0.7	0.8 ± 0.3
	Ga XPS	370	7.5	0.75 ± 0.10	0.7	0.9 ± 0.4
	Al XPS	1287	16.5	0.25 ± 0.07	0.7	1.0 ± 0.4
$In_xAl_{1-x}As$ grown at 480°C	Al AES	66	5.0	0.35 ± 0.07	0.52	0.8 ± 0.2
	In AES	401	9.6	0.82 ± 0.20	0.52	1.7 ± 0.7
	In XPS	1042	15.0	0.53 ± 0.07	0.52	0.7 ± 0.4
	Al XPS	1287	16.5	0.36 ± 0.05	0.52	1.4 ± 0.3
$In_xAl_{1-x}As$ grown at 480°C and annealed at 520°C	Al AES	66	5.0	0.75 ± 0.20	0.52	0.0 ± 0.4
	In AES	401	9.6	0.41 ± 0.10	0.52	0.2 ± 0.4
	In XPS	1042	15.0	0.19 ± 0.06	0.52	-1.2 ± 0.4
	Al XPS	1287	16.5	0.62 ± 0.15	0.52	-0.2 ± 0.7
$In_xGa_{1-x}As$ grown at 480°C	Ga AES	55	5.0	0.25 ± 0.06	0.53	1.1 ± 0.2
	In AES	401	9.6	0.68 ± 0.20	0.53	1.2 ± 0.7
	Ga XPS	370	7.5	0.36 ± 0.10	0.53	0.9 ± 0.3
	In XPS	1042	15.0	0.62 ± 0.10	0.53	1.1 ± 0.6
$In_xGa_{1-x}As$ grown at 480°C and annealed at 520°C	Ga AES	55	5.0	0.41 ± 0.15	0.53	0.4 ± 0.3
	In AES	401	9.6	0.49 ± 0.15	0.53	0.5 ± 0.5
	Ga XPS	370	7.5	0.52 ± 0.12	0.53	0.6 ± 0.4
	In XPS	1042	15.0	0.40 ± 0.10	0.53	0.0 ± 0.6
$In_xGa_{1-x}As$ grown at 480°C	Ga AES	55	5.0	0.47 ± 0.15	0.2	0.9 ± 0.3
	In AES	401	9.6	0.29 ± 0.20	0.2	0.6 ± 0.4
	Ga XPS	370	7.5	0.59 ± 0.15	0.2	0.8 ± 0.5
	In XPS	1042	15.0	0.27 ± 0.10	0.2	0.6 ± 0.5
$In_xGa_{1-x}As$ grown at 480°C and annealed at 520°C	Ga AES	55	5.0	0.68 ± 0.20	0.2	0.5 ± 0.5
	In AES	401	9.6	0.22 ± 0.07	0.2	0.3 ± 0.3
	Ga XPS	370	7.5	0.62 ± 0.10	0.2	0.2 ± 0.3
	In XPS	1042	15.0	0.23 ± 0.05	0.2	0.4 ± 0.3

B. Heterointerfaces

Surface segregation in heterostructures is now considered. We have built heterostructures of all three types and analyzed their surface in search of atoms normally belonging to a buried layer. As opposed to the case of

ternary alloys, we clearly deal here with a transitory regime. We modelize the segregation process in a type-II $B\text{-As}/A\text{-As}$ heterostructure where A tends to segregate atop $B\text{-As}$ in the following phenomenological manner based on the very low bulk mobility; the physical basis of this model will be discussed further on. We assume that

TABLE II. Surface composition of ternary alloys x_s obtained from measurements on these materials (TA) and corresponding predictions obtained from measurements in heterojunctions (HJ) with Eq. (6) and mean values from Table IV; the tendencies to surface segregation (E_s) deduced from TA values are also indicated. LT and HT refer to growth temperatures and to temperatures above the In desorption threshold ($\approx 550^\circ\text{C}$).

T	Alloy	x_b	$x_s(\text{TA})$	$x_s(\text{HJ})$	E_s
LT	$Ga_xAl_{1-x}As$	0.70	1.1 ± 0.3	0.79	Ga > Al
	$In_xAl_{1-x}As$	0.52	1.3 ± 0.3	0.98	In > Al
	$In_xGa_{1-x}As$	0.53	1.1 ± 0.3	0.90	In > Ga
	$In_xGa_{1-x}As$	0.20	0.7 ± 0.3	0.84	In > Ga
HT	$In_xAl_{1-x}As$	0.52	-0.3 ± 0.3		
	$In_xGa_{1-x}As$	0.53	0.4 ± 0.3		
	$In_xGa_{1-x}As$	0.20	0.3 ± 0.3		

segregation processes involve only two monolayers: the top one of the heterostructure under growth and the one being deposited. During the deposition of the first monolayer of *B*-As on *A*-As, a fraction σ_1 of the top *A* monolayer segregates to the surface, thus burying the same fraction of the deposited *B*-As monolayer. The process goes on at each *i*th deposited monolayer, with an efficiency σ_i . The composition profile x_i in the *A* element of the *i*th monolayer (depth $z = ib$) after the deposition of *n* monolayers is then

$$\begin{aligned} x_i &= 1, \quad i \leq 0 \\ x_i &= 1 - \sigma_1 (=1 - \sigma), \quad i = 0 \\ x_i &= (1 - \sigma_{i+1}) \prod_{j=1}^i \sigma_j [= (1 - \sigma)\sigma^i = (1 - \sigma)e^{-z/\tau}], \quad 0 < i < n \\ x_i &= \prod_{j=1}^n \sigma_j (= \sigma^n), \quad i = n \end{aligned} \quad (3)$$

where in the parenthetical expressions all σ_i are taken to be identical ($\equiv \sigma$) as a first-level approximation. In this description, the top *A* monolayer is distributed in the *B*-As layer with an exponential gradient, leading to an interface thickness scaled by τ ($= -b/\ln\sigma$), and a $(1 - \sigma)$ composition at the interface. Since only this monolayer is involved, type-II or type-III heterostructures give the same composition profile. With the model described above for the probing depth of analysis techniques, we obtain the expected dependence of the reduced ratio *R* for the segregating atom *A* with the deposited thickness *nb* for a type-II heterostructure:

$$\begin{aligned} R_A(\text{II}) &= (1 - e^{-b/L}) \sum_{i=-\infty}^{i=n} x_i e^{-(n-i)b/L} \\ &= \epsilon^{n+1} + \epsilon^n(1 - \epsilon)(1 - \sigma) \\ &\quad \times \left[1 - \frac{\sigma^n}{\epsilon^n} \right] / \left[1 - \frac{\sigma}{\epsilon} \right] + \sigma^n(1 - \epsilon). \end{aligned} \quad (4)$$

The three terms of this expression correspond, respectively, to the *B*-As underlayer, the overlayer, and the surface. For type-III heterostructures, *R*(III) is similar to *R*(II) except for the missing first term. Type-I heterostructures are type-II ones with $n = 1$. Corresponding expressions may be easily derived for the reduced ratios involving the nonsegregating atom.

We first consider the results for type-I heterostructures (Table III). For the GaAs/AlAs, InAs/GaAs, and InAs/AlAs heterostructures, the agreement between experimental and theoretical values obtained for a model without segregation ($\sigma = 0$) is correct, considering the roughness of the model. On the other hand, the discrepancies in GaAs/InAs and AlAs/InAs systems exceed the experimental accuracy, and systematically indicate an excess of substrate atoms at the surface. The agreement is much better if we suppose a complete exchange ($\sigma = 1$). Finer determinations of σ (Table III) are given by the following relations, which are deduced like relations (4) but where different lattice parameters for *A*-

As and *B*-As layers have been taken into account [see model in Fig. 1(b)]:

$$\begin{aligned} \sigma &= \frac{1 - \epsilon_A - R_A(\text{II})}{(1 - \epsilon_A)(1 - \epsilon_B)} \\ &= \frac{R_B(\text{II}) - \epsilon_A}{(1 - \epsilon_A)(1 - \epsilon_B)}. \end{aligned} \quad (5)$$

Average σ values where the weight of data decreases with increasing electron escape depth are listed in Table IV. For GaAs/InAs and AlAs/InAs, and InAs/GaAs and InAs/AlAs, we obtain tendencies to, respectively, near-total and near-null segregation efficiencies; no significant segregation is detected in AlAs-GaAs couples.

For InAs/AlAs/InAs and GaAs/InAs/GaAs type-III structures, we probed the decay of surface-sensitive AES peaks corresponding to the interlayer atoms with overlayer thickness. These data are compared in Fig. 4 to

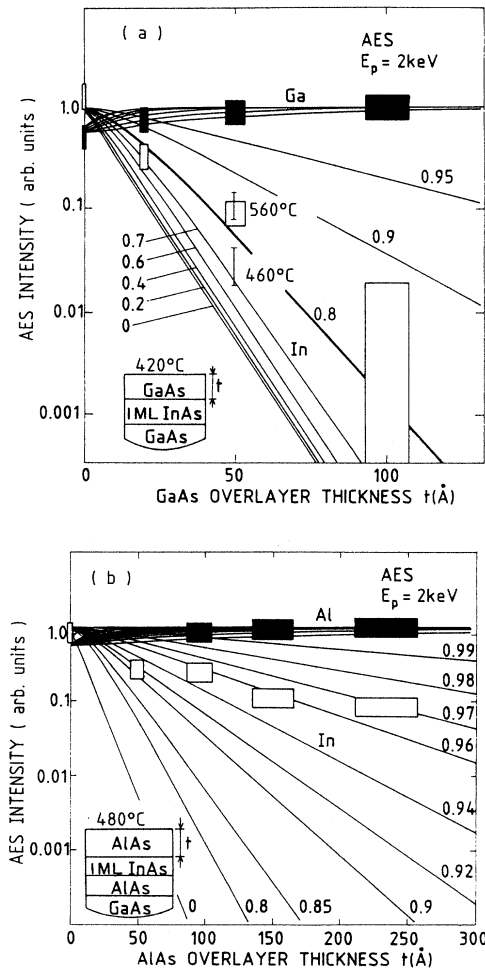


FIG. 4. Evolution of AES signals in type-III heterostructures (a) GaAs/InAs/GaAs and (b) AlAs/InAs/AlAs with thickness of the final layer. Values are normalized to the signal corresponding to the absence of final layer. Bars in (a) are calculated from data of Ref. 27 obtained at different growth temperatures. Solid lines are model predictions for various σ values according to Eq. (4).

TABLE III. AES-XPS results for type-I structures; for each peak, the electron escape depth and the reduced ratio averaged over 3–10 samples are listed, together with the value of the segregation coefficient σ deduced from relations (5).

Type-I structure	Peak	L (Å)	R	σ
1 ML InAs/GaAs 6.06 Å-5.65 Å	Ga AES	5.0	0.53±0.10	-0.08±0.50
	Ga XPS	7.5	0.73±0.12	0.58±1.00
	In AES	9.6	0.34±0.08	-1.00±1.10
	In XPS	15.0	0.19±0.02	-0.22±0.60
	Ga XPS	19.5	0.86±0.03	0.20±1.50
	In XPS	19.5	0.18±0.03	-1.80±1.50
1 ML GaAs/InAs 5.65 Å-6.06 Å	Ga AES	5.0	0.21±0.10	1.13±0.50
	Ga XPS	7.5	0.21±0.07	1.00±0.70
	In AES	9.6	0.80±0.08	0.80±1.10
	In XPS	15.0	0.84±0.05	0.37±1.50
	Ga XPS	19.5	0.11±0.02	1.28±1.00
	In XPS	19.5	0.90±0.05	1.80±2.50
1 ML InAs/AlAs 6.06 Å-5.65 Å	Al AES	5.0	0.54±0.10	0.03±0.50
	In AES	9.6	0.24±0.05	0.44±0.70
	In XPS	15.0	0.17±0.02	0.41±0.60
	Al XPS	16.5	0.99±0.04	5.98±1.50
	In XPS	19.5	0.17±0.03	-1.34±1.50
1 ML AlAs/InAs 5.66 Å-6.06 Å	Al AES	5.0	0.26±0.10	0.88±0.50
	In AES	9.6	0.95±0.12	2.97±1.80
	In XPS	15.0	0.84±0.05	0.38±1.60
	Al XPS	16.5	0.13±0.02	1.04±0.70
	In XPS	19.5	0.89±0.04	1.29±2.00
1 ML AlAs/GaAs 5.66 Å-5.65 Å	Ga AES	5.0	0.59±0.10	0.12±0.50
	Al AES	5.0	0.60±0.12	-0.90±0.70
	Ga XPS	7.5	0.57±0.08	-1.17±0.80
	Al XPS	16.5	0.13±0.03	1.11±1.20
	Ga XPS	19.5	0.87±0.03	0.28±1.50
1 ML GaAs/AlAs 5.65 Å-5.66 Å	Ga AES	5.0	0.40±0.10	0.17±0.50
	Al AES	5.0	0.61±0.10	0.22±0.60
	Ga XPS	7.5	0.33±0.03	-0.16±0.30
	Al XPS	16.5	0.85±0.05	0.30±2.00
	Ga XPS	19.5	0.14±0.03	0.70±1.20

TABLE IV. Summary of segregation efficiencies σ and interface thicknesses τ at heterojunctions deduced from various measurements and structures.

Structure	Type	Technique	σ	τ (Å)	E_s
InAs/GaAs	I	AES-XPS	-0.10±0.60	< 4	In > Ga
GaAs/InAs	I	AES-XPS	1.10±0.40	> 8	In > Ga
	III	AES-XPS	0.80±0.08	10–25	In > Ga
	III	RBS	0.80±0.10	8–30	In > Ga
	I	AES-XPS	-0.10±0.70	< 6	In > Al
AlAs/InAs	I	AES-XPS	1.30±0.70	> 6	In > Al
	III	AES-XPS	0.95±0.03	35–150	In > Al
GaAs/AlAs	I	AES-XPS	0.00±0.70	< 8	Ga = Al
AlAs/GaAs	I	AES-XPS	0.20±0.30	< 4	Ga ≥ Al
	I	UPS	0.30±0.50	< 8	Ga ≥ Al
	II	AES-XPS	< 0.60	< 6	Ga ≥ Al

those predicted for various σ values. The values giving the best fit (Table IV) are in fair agreement with the ones obtained from type-I structures, and their accuracy is better for near-unity σ values. These results show that, when segregation takes place, atom exchanges proceed therefore far from the planned interface. The differences between experimental and theoretical curves (Fig. 4) even indicate a slight increase of σ with thickness ($\sigma_{i+1} \geq \sigma_i$). For the AlAs/GaAs/AlAs type-III structure, surface Ga segregation was expected from our results for ternary compounds and from Ref. 11. However, we did not observe significant AES or UPS Ga peaks at AlAs overlayer thicknesses above 50 Å, showing that σ is less than 0.6.

We have confirmed this analysis by RBS studies of type-III heterostructures (100 Å GaAs/1 ML InAs/GaAs) which will be reported in detail elsewhere.²⁴ Minimum channeling yields in both (100) and (110) directions show that atoms in the whole heterostructure are approximately located at the substrate positions. This should not be the case since the InAs monolayer should create a stacking fault visible in off-normal directions. It is therefore redistributed in the GaAs overlayer. Fits of angular scans of indium yield using redistribution profiles described by (4) give $\sigma = 0.8 \pm 0.1$ and $\tau \approx 15$ Å, in agreement with the AES-XPS determination. Finally, photoluminescence experiments performed on neighboring type-III structures^{4,25} lead to similar conclusions. High-resolution microscopy of these structures²⁶ also indicates indium redistribution, though the concentration gradient at the GaAs/InAs interface is different from a mere exponential tail. Again for the case of GaAs/InAs, we have determined the influence of various parameters on σ . From previous data²⁷ processed like ours (Fig. 4), we infer that σ does not depend significantly on T from 420 °C to 560 °C, and separate experiments also show that it does not depend either on the growth rate of the GaAs overlayer, from 0.1 to 1 $\mu\text{m/h}$. Finally, we also investigated the influence of the compressive strain imposed on the In atoms in various heterostructures with different base substrates (GaAs, $\text{Ga}_{0.53}\text{In}_{0.47}$, InP). For compressions ranging from 0% to 7%, we observed a slight decrease of σ with increasing compression (Fig. 5).

σ and τ values deduced from all our data are summarized in Table IV. Thicknesses τ smaller than 1 ML ($\tau < 3$ Å; $\sigma < 0.4$) indicate intermixing limited within the first monolayer. The tendency to surface segregation is given by $\text{In} > \text{Ga} \geq \text{Al}$. Within the phenomenological model described above, we expect the segregation process in $A_xB_{1-x}\text{As}$ ternary alloys to be limited to the top layer and the stationary surface concentration x_s and reduced ratio R_A to be

$$\begin{aligned} x_s &= x_b + \sigma(1 - x_b), \\ R_A &= x_b + \sigma(1 - \epsilon)(1 - x_b). \end{aligned} \quad (6)$$

The situations in ternary alloys and heterostructures are different since in the former case atoms of the segregating species are continuously added to the surface while in the latter case only segregated atoms are present. However, we check that σ values obtained in heterostructures give x_s values for ternary alloys in agreement with experimen-

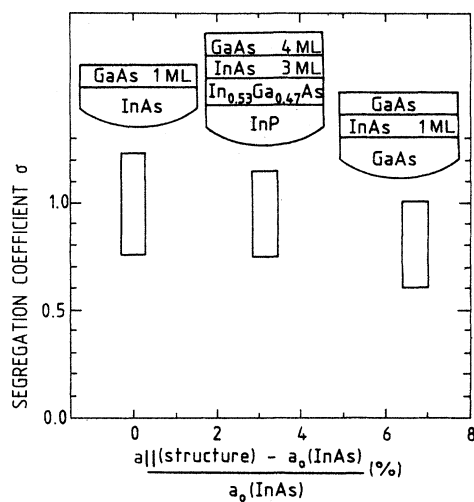


FIG. 5. Evolution of the segregation efficiency σ of In in various structures with the in-plane deformation $\delta a/a$ applied to the InAs lattice. Rectangles indicate the uncertainties on σ values. Structures sketched above each rectangle are planned structures which would be observed if no segregation took place. Actual structures are different due to In segregation from the next-to-last InAs layer to the last GaAs layer but retain the strain induced by the underlying layers ($\text{In}_{0.53}\text{Ga}_{0.47}\text{As}$ for the center structure and GaAs for the left-hand one) due to pseudomorphism.

tal values (Table II) except possibly for the Ga segregation in Ga-Al-As systems.

V. DISCUSSION

A. Growth-induced stationary state and thermodynamical equilibrium

From a thermodynamical point of view, the ideal surface segregation experiment involves a system formed by a bulk phase (semi-infinite solid alloy $M_{1-x}N_x$ of x_b composition), a surface phase (surface of the latter with a x_s composition), and a gas phase (atmosphere of M and N under their gaseous form). Thermodynamical equilibrium requires the adjustment of x_b, x_s and of the partial pressures of M and N in the atmosphere. This ideal situation is seldom found. Most experiments in metals do not involve a gas phase, and only consider the bulk-surface equilibrium reached after annealing samples cleaned or fractured under vacuum. If the annealing temperature is high enough and its duration long enough, i.e., if the diffusion path of the segregating species is long enough, the surface-subsurface concentration equilibrium is reached and the subsurface region depleted by the segregation process recovers its bulk composition. In this situation, the composition gradient at the surface is found to be very rapidly decreasing (and eventually oscillating) across the topmost atomic layers. This sharp gradient allows us to consider the top layer as the surface phase and its composition as the surface composition x_s . Many experimental and theoretical studies have been devoted to

the relation between x_b , x_s , the temperature, the crystallographic orientation of the surface, etc.

Performing similar (vacuum) annealing experiments in A - B - As semiconductor compounds is not possible since long enough diffusion paths cannot be obtained in reasonable times except at temperatures ($> 1000^\circ\text{C}$) where the material rapidly evaporates. This evaporation could be counteracted by an adequate (A, B, As) atmosphere as in the "ideal" experiment, but its pressure would be too high for practical feasibility. The actual growth experiment differs from this "ideal" one in two ways: (1) the (A, B) partial pressures in the gas phase are in the ($x_b, 1-x_b$) proportion but are larger than the ones which match the bulk composition in terms of chemical potential (this excess causes the growth); and (2) the temperature is not high enough to allow any significant bulk diffusion. We now consider whether these differences prevent the system from reaching an equilibrium configuration.

We take the surface under growth, which is moving in the laboratory coordinates, as the origin of depth z . We define the surface as the region ($z < z_s \approx 5 \text{ \AA}$) where atom movement is possible and the bulk ($z > z_s$) as the region where the atoms are frozen. In the surface region, the concentration is taken to be constant. Several characteristic times must be considered: t_{equil} the time needed for the incoming atoms to achieve local equilibrium in the surface region, t_{growth} the time needed to grow a thickness equal to the surface thickness ($=z_s/V_{\text{growth}}$), t_{stat} the time needed to reach a stationary state with respect to surface and bulk compositions starting from the binary substrate, and t_{obs} the total growth duration before observation.

We first show that the bulk composition near the surface ($z = z_s$) is consistent and equal to the desired value x_b . When a stationary regime is attained ($t_{\text{obs}} > t_{\text{stat}}$), A and B atoms coming from the gas phase only transit through the surface region before incorporating in the bulk; no accumulation in the surface exists and the bulk composition for $z > z_s$ is constant, and hence uniform ($=x_b$) since growth proceeds. If segregation does occur, the x_s^* stationary value is larger than x_b but may be different from the equilibrium value x_s obtained in the ideal experiment. The excess surface concentration $x_s^* - x_b$ is built up during the transitory regime from a depletion of the bulk concentration $x(z_s^+) - x_b$. In other words, in this regime the incorporation into the bulk is smaller for the segregating species. The conservation relation for this species can be written as

$$x_s^* - x_b + \int_0^{t_{\text{stat}}} \frac{x(z_s^+, t) - x_b}{t_{\text{growth}}} dt = 0. \quad (7)$$

It is then clear from (7) that $x(z_s^+) - x_b$, i.e., all the transient composition gradient, is either always small or high only during a time t_{stat} of the order of t_{growth} which is much smaller than t_{obs} , and hence raises no problem in any case for the bulk concentration of the sample we observe. However, if in the second case t_{stat} is much smaller than t_{obs} , meaning that the build-up of the surface ex-

cess composition is so rapid that we always observe the stationary composition x_s^* , in the first one we could observe at t_{obs} a surface composition not yet built up and hence smaller than x_s^* . This does not seem to be the case because we do not see a significant variation of the measured x_s with $t_{\text{obs}} > 300t_{\text{growth}}$ and because the mechanisms involved in the heterojunction formation which are similar to those involved in the transitory regime are stationary after less than $50t_{\text{growth}}$, i.e., well below the t_{obs} considered here. The observed surface composition is then indeed the stationary composition x_s^* .

Considering now the possible difference between x_s and x_s^* , it may be noted that we do not observe significant variations of σ in heterojunctions with temperature or growth rate, which indicates that the surface segregation reaction is not time limited ($t_{\text{equil}} < t_{\text{growth}}$). In other words, the growth rate of less than 1 ML/s is a slow one with respect to the segregation mechanisms and we deal with a quasiequilibrium for the phenomenon considered, even though the partial pressures are considerably higher than the genuine equilibrium pressures which give a zero growth rate. We then estimate $t_{\text{equil}} < t_{\text{growth}} < t_{\text{stat}} < t_{\text{obs}}$. This first indicates that the growth interruption at t_{obs} should not perturb x_s^* : the shutter action is much faster than t_{growth} and no bulk-surface redistribution should occur after that since local equilibrium is already reached. Then the system at t_{obs} is a quasi-semi-infinite and homogeneous bulk with a concentration x_b and a surface which is kept in local equilibrium with this underlying bulk at a concentration x_s by the fast surface-located exchanges. Finally, we conclude that even though the equilibrium is not reached by the usual means, the x_s values obtained here are nevertheless similar to the ones which would be obtained in the hypothetical "ideal experiment." For similar reasons, x_s values deduced from ternary compounds or from the heterojunctions through σ are identical. We may then discuss them in first approximation with models developed for metals and involving a bulk-surface thermodynamical equilibrium.

B. Surface segregation models

Thermodynamically, surface segregation in vacuum stems from the balance of chemical potentials of the segregating atom in the bulk and at the surface, just like adsorption stems from the balance of chemical potentials in the gas phase and at the surface. If the movement of one atom (A in an AB alloy) from the bulk to the surface yields a positive energy E_s , chemical potentials in bulk and surface regions are not equal for a homogeneous concentration; the equilibrium surface concentration x_s is then higher than the concentration x_b of the bulk which feeds it. The most simple quantitative model of segregation involves only the entropy term and the "chemical" energy E_s as contributions to the free energy, and the balance of chemical potentials is written as McLean's equation:⁷

$$\ln \left[\frac{x_s}{1-x_s} \right] + \frac{E_s}{kT} = \ln \frac{x_b}{1-x_b} . \quad (8)$$

This relation has been checked to hold in many systems,⁷ at least for low x_b . In our case, we must also introduce a

$$\ln \left[\frac{x_s}{1-x_s} \right] + \frac{E_s}{kT} + \frac{Ca^3}{4kT} \left[\frac{\delta a}{a} \right]^2 \left[1 + \frac{\delta a}{a} (x_s + x_b)(x_s - x_b) \right] = \ln \frac{x_b}{1-x_b} , \quad (9)$$

where C is the mean elastic constant, a the bulk parameter, and $\delta a/a$ the parameter difference between pure A and pure B materials. The scaling elastic factor $Ca\delta a^2/4kT$ may be estimated, for instance for the In-Ga-As system, to be ≈ 2 at 800 K for $C \approx 0.6$ eV/Å³ (Ref. 23) and $\delta a/a \approx 0.07$. From this relation, the variation of x_s with x_b and T may be predicted, E_s being the only unknown parameter. In Fig. 6, we plot the experimental $x_s(x_b)$ values obtained from XPS data on In_{*x*}Ga_{1-*x*}As alloys, together with predictions of Eq. (9) for various values of the energy parameter E_s/kT at $T = T_{\text{growth}} \approx 750$ K. Comparison between theory and experiment yields $E_s \approx 0.15 \pm 0.1$ eV. The same data for Ga_{*x*}Al_{1-*x*}As alloys yields $E_s = 0.1 \pm 0.05$ eV. It may be noted that the stronger segregation energy for In in In_{*x*}Ga_{1-*x*}As than for Ga in Ga_{*x*}Al_{1-*x*}As correlates well with the higher tendency to segregation at the heterointerfaces expressed by the higher σ value (Sec. IV B, Table IV). These values in turn allow us to determine the variation of x_s with T for given alloys (Ga_{0.7}Al_{0.3}As and In_{0.5}Ga_{0.5}As in Fig. 7). For these rather high x_b values ($x_b \geq 0.5$), x_s decreases with T from 1 to x_b but rather slowly, in agreement with the experimental results which show no significant dependence of $\sigma(x_s)$ on T over a ≈ 100 -K range. Actually, for the rather high x_b and the rather low temperatures involved, the chemical potential in the bulk phase and the segregation energy are too high to be counteracted by disorder or elastic strains and x_s is always almost unity. Under the normal growth conditions, the only way to change x_s is then desorption (Fig. 2, Tables I and II) whose activation energy is comparable to E_s but which involves a chemical potential in the neighboring phase (a pure As atmosphere) considerably lower.

Finally, we may use Eq. (9) with the E_s values determined above in order to model concentration profiles at heterojunctions. We assume that at the deposition of every monolayer, the concentrations of the segregating element in this monolayer and in the underlying one reach an equilibrium according to the $x_s(x_b)$ relation (9) obtained in ternary alloys and to the matter-conservation relation. The underlying monolayer is then “frozen” for the rest of the growth. Concentration profiles obtained by this method for GaAs/AlAs and GaAs/InAs heterojunctions and GaAs/InAs short-period superlattices are shown in Fig. 8. It may be seen here that the two interfaces behave differently: the one with the segregating element atop (“inverted” in the MBE terminology) is nar-

rower but rougher than the other one (“normal”). The model considered here is similar to the cruder one used to derive relations (3), where $x_s(x_b)$ was taken as $x_s = \sigma x_b$ (regular solution approximation) and where we assume the absence of atom redistribution following the deposition of the segregating species on the other one. Considering the $x_s(x_b)$ shape in Fig. 6, this approximation is

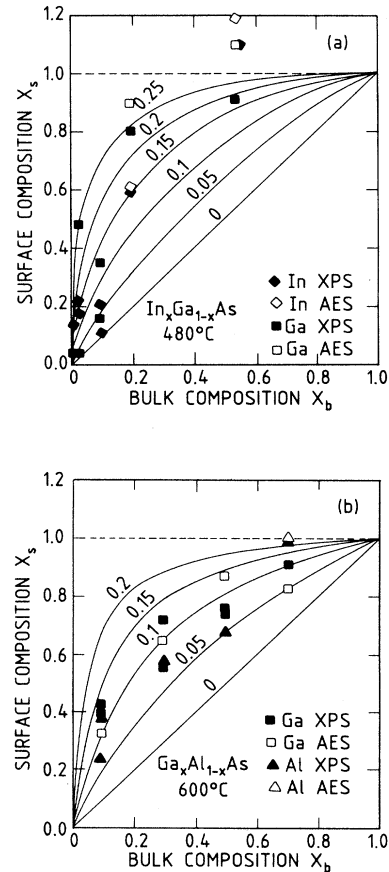


FIG. 6. Experimental segregation isotherms $x_s(x_b)$ for (a) the In_{*x*}Ga_{1-*x*}As alloys at 480°C and (b) Ga_{*x*}Al_{1-*x*}As alloys at 600°C, including the data of Table II and theoretical expectations from Eq. (9) with various values of the energy term E_s (indicated in eV). The elastic scaling factor $Ca\delta a^2/4kT$ is 2 for In_{*x*}Ga_{1-*x*}As and 0 for Ga_{*x*}Al_{1-*x*}As. Typical uncertainties of experimental data are listed in Table I.

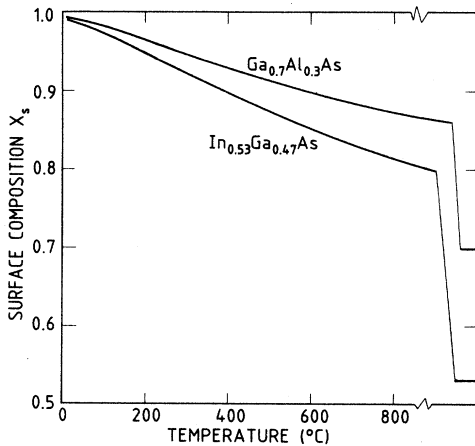
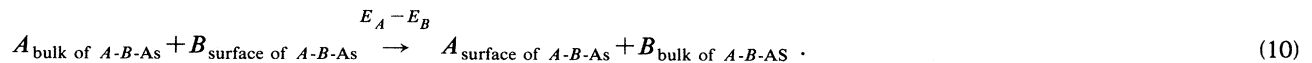


FIG. 7. Expected dependence of x_s on growth temperature for selected alloys; curves are obtained from Eq. (9) with the elastic and energy factors deduced from Fig. 6.

correct for $x < 0.2$, i.e., for most of the concentration gradient in the heterojunctions considered in our experiments; the present analysis also confirms the $\sigma = 0.8$ value adopted from Table IV for GaAs/InAs, but would indicate a higher value for GaAs/AlAs (0.5 instead of 0.3).

C. Surface segregation and surface-bulk exchange reactions

Besides the energy of the segregation, we may also consider why a given atom segregates rather than another

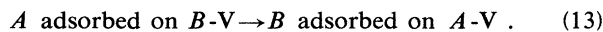


The direction and extent of the segregation is linked to $E_A - E_B$ and hence to the order of the various E . From literature data and ours, this order is

$$E_{\text{In}} > E_{\text{Ga}} \geq E_{\text{Al}} \quad (\text{arsenide alloys and heterostructures}), \quad (11)$$

$$E_{\text{Ga}} < E_{\text{Al}} \quad (\text{antimonide heterostructures}). \quad (12)$$

Whatever the bulk composition, we observe always the segregation of one of the components and not of the other, so that the order for III-V heterostructures is intrinsic to the third-column arsenides. Similar observations can be made in neighboring reactions known as exchange reactions observed during the deposition of a third-column metal on a III-V compound:



With similar definitions, the same experimental E order for metals on arsenides and phosphides is found in most experiments (see a review of this field in Ref. 29). The ex-

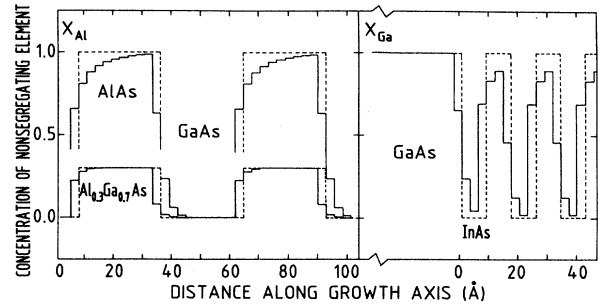
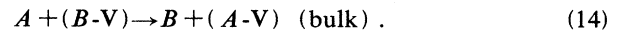


FIG. 8. Profile of composition in nonsegregating element for selected $\text{Ga}_x\text{Al}_{1-x}\text{As}/\text{GaAs}$ heterostructures (Ga segregation) and for a 3 ML InAs/3 ML GaAs short-period superlattice grown on a GaAs substrate (In segregation). Each step corresponds to a monolayer. Planned profiles are the dotted lines. Actual profiles are calculated according to the model of Sec. V B, with the following parameters for Ga/Al (In/Ga) segregation: segregation energy $E_s = 0.1$ eV (0.15 eV), scaling elastic factor $C a \delta a^2 / 4kT = 0$ (2), $b = 2.83$ Å (3.03 Å), lattice mismatch $\delta a/a = 0$ (0.07), and growth temperature $T = 900$ K (750 K). Please note the difference between “normal” and “inverted” GaAs/Ga $_x$ Al $_{1-x}$ As interfaces.

one, i.e., what is the driving force for surface segregation. If we define the tendency to surface segregation of an atom A as the energy gain E provided when it moves from the bulk to the surface, A will segregate to the surface of the A - B -As alloy if the following reaction takes place:

tent of these exchanges has also been claimed³⁰ to be correlated with the heat of bulk reactions such as



Finally, all reactions involving surface-bulk exchanges in III-V semiconductors yield similar orders for energies E . It should be kept in mind, however, that (10) involves bonds with fifth-column elements and not (13). For instance, if the exchange of free Al atoms with the Ga atoms of GaAs is easy even at room temperature, it is no proof of the likeliness of similar reactions when Al atoms are surrounded by As atoms in the surface plane. Furthermore, for the various reactions considered, the energies associated with surface configurations like reconstruction, which may contribute significantly to the energy balance, are *a priori* very different, and are not even taken into account in (14).

The origin of the driving force for segregation and hence of the E order is then not clear at present though some explanations have been proposed.^{9,11,31} Correlations with bulk bonding energies (the atom which is the

more strongly bonded comes to the surface) have been put forward. Indeed, the bonding-energy order¹

$$\text{In-As}(1.41 \text{ eV}) < \text{Ga-As}(1.59 \text{ eV}) < \text{Al-As}(1.98 \text{ eV}) , \\ \text{Ga-Sb}(1.50 \text{ eV}) < \text{Al-Sb}(1.79 \text{ eV})$$

is the same as the E order for arsenides, but not for antimonides. It has also been suggested that elastic strains play the first part (the biggest atom comes to the surface). Indeed, we find a bond length order¹ similar to the E order:

$$\text{In-As}(2.62 \text{ \AA}) > \text{Ga-As}(2.45 \text{ \AA}) \approx \text{Al-As}(2.45 \text{ \AA}) , \\ \text{Ga-Sb}(2.64 \text{ \AA}) < \text{Al-Sb}(2.66 \text{ \AA}) .$$

In this model, we should expect a variation of E and hence possibly of $x_s(x_b)$ or σ with the state of strain of the substrate, which we do not observe in GaAs/InAs (Fig. 5). Other correlations with the incorporation energy or the surface diffusion coefficient have also been put forward. However, such quantities, just like bonding energies or covalent radii, are expected to follow somehow the Periodic Table order for compounds with a same fifth-column element and these correlations may be only useful as first-basis predictions for future systems. Furthermore, some puzzling experiments and theories on segregation in metal alloys³² show that the prediction of the segregating component is by no means straightforward and may be reversed, for instance by changing the crystal orientation of the surface, when conflicting effects like atom size (surface strain) and pair-interaction (surface energy) are opposed. It may also be stressed again that all possible effects are connected in some way with the surface relaxations and/or reconstruction which are not taken into account in present theories.

D. Microscopic mechanisms

Our experiments show that the microscopic mechanism leading to the segregation is rapid with respect to the growth, i.e., the exchange rate is so fast that the efficiency of the segregation process is not limited by kinetics in usual conditions. This is expected since this mechanism is probably similar to surface diffusion which is known to be fast enough to insure the correct incorporation in the bulk lattice and the surface smoothening. Like any atom movement at the surface, it is likely to occur preferentially at defects which are the only sites where the reaction can proceed by successive movements without any direct atom exchange.³³ Indeed, the extent of (13) reactions strongly depends also on the roughness of the substrate: it is low (null?) on (110) well-cleaved surfaces and high on band cleavages or on (100) surfaces,³⁴ which indicates that substrate defects (mainly steps) are the necessary sites where the reaction takes place. In our case, the insensitiveness to growth conditions suggests that extrinsic defects (dislocations, growth steps, etc.) are not involved, but rather intrinsic ones such as surface vacancies or steps associated with the surface reconstruction. Finally, it may be mentioned that the segregation mechanism is rather efficient, as seen from

the high σ values: a monolayer can be transported over considerable thicknesses. The limitation and possibly also the increase at large overlayer thicknesses of this efficiency may possibly arise from extended surface roughnesses and/or from composition unhomogeneities in the surface plane, i.e., 2D clustering or alloy phase separation.

VI. CONSEQUENCES OF SEGREGATION PROCESSES

From the point of view of the structures obtained by MBE growth, it may be first pointed out that, if segregation processes may raise a problem in the transitory regime, they are necessary in the stationary regime, for instance for ternary alloys where the surface is constantly regenerated at a composition x_s different from the bulk one x_b set by the ratio of input atom fluxes. As mentioned in the Introduction, the problem is more acute at heterointerfaces. The picture we obtain of their build-up is the following. Foreign atoms are sent on a substrate; before getting buried by the impinging flux, they stay at the surface long enough to travel sizeable distances (up to 1 μm for common growth rates), and to seek for lower-energy configurations. If a driving force is provided, an exchange between the impinging atoms and the substrate atoms is promoted, probably at defects. When the segregation efficiency is high ($\sigma \approx 1$), the process may repeat all along the overlayer growth. A thin layer of the substrate material then "floats" on the growing overlayer. This also occurs if the solubility of the substrate atoms in the overlayer material is low. In either case, the final structure is the one desired, except for a 1-ML error at the start and the end. It may be pointed out that even a very slow dissolution can lead to very high doping levels if the segregating atoms acts as dopants: if imperfections in the segregation leave 0.001 ML of substrate atoms to be incorporated in each growing monolayer, the supply is exhausted after a 0.3- μm growth, but the resulting overlayer has a doping level of $3 \times 10^{19} \text{ cm}^{-3}$. On the other hand, if the segregation is weak ($\sigma \ll 1$), the segregated atoms dissolve rather rapidly in the overlayer. An interfacial ternary alloy appears, with a composition gradient of thickness scaled by $-b/\ln\sigma$ (5 \AA for $\sigma=0.5$, 30 \AA for $\sigma=0.9$, 300 \AA for $\sigma=0.99$).

Another result of segregation is the decrease of the geometrical accuracy of the final structure (see Fig. 8). Suppose we build on a substrate A -As alternating layers of A -As and B -As. If segregation occurs at the deposition of A -As on B -As with $\sigma \approx 1$, the final structure is as planned, except for its surface which is always A -As, even when the last layer deposited is B -As. It is the same if the segregation takes place at the deposition of B -As on A -As, but in addition the thickness of the first B -As layer is too thin by one monolayer. This may be a nuisance if this layer is only several monolayers thick and plays an important part in the structure (quantum well, or short-period superlattice). Such effects have been observed in GaAs/InAs/GaAs structures by luminescence studies.^{4,25} The case where σ is significantly less than unity is no less bothering since an interface roughness is generated,

which cancels the advantage of starting flat surface. From a more general point of view, since the segregation reaction is operative only for one of the depositions, A -As on B -As or B -As on A -As, A -As/ B -As and B -As/ A -As interfaces cannot be similar. It has been suggested, among other explanations, that this was the origin of the differences between GaAs/Ga_{0.7}Al_{0.3}As "normal" and "inverted" interfaces.⁸

Besides the roughening of interfaces, segregation has further consequences. First, in the case of the "floating" substrate layer, the sample surface is not formed by the overlayer material, as could be expected. Indeed, it has most of the properties of the substrate surface, electronic ones included;²⁰ this may be important if these properties must be put into use (low surface recombination, chemical passivation, further grown, etc.). For instance, the (temperature, arsenic pressure) "MBE phase diagram," which separates the "group-III-rich" or "As-rich" growth conditions, is a surface property: two monolayers of InAs on InP have the same "phase diagram" as bulk InAs.²⁰ Therefore, the growth conditions should be set in principle with respect to the actual surface and not to the presumed overlayer material surface. Again, this may be important in short-period structures where pattern sizes are such that growth can never be considered as stationary.

Finally, segregation has a number of consequences, most of them negative with respect to the quality of the interface. A positive consequence is the possibility of obtaining monoatomic layers without having to build them with atom fluxes, with possible applications to atomic-layer epitaxy: the reaction can potentially stop exactly at the completion of the monolayer whatever the growth conditions. However, much work must still be performed before putting segregation into actual use and the present problem is rather to get rid of it, by energetic or kinetic means. If thermodynamic equilibrium of a given structure needs to be maintained, segregation equation (9) with $E_s \approx 1$ eV shows that reducing significantly the segregation would need too high temperatures ($\gg 1000^\circ\text{C}$) for practical purposes. On the other hand, we may also try to reduce segregation by changing its kinetics with the counterpart of getting off-equilibrium interfaces. From our results, it seems that t_{growth} cannot be decreased (i.e., V_{growth} increased) below current t_{equil} since the process is too fast. Then we may try to increase t_{equil} , which is linked to the microscopic processes, by decreasing the mobility of atoms at the surface, the number of reaction sites, and/or the rate of exchange at these sites. The temperature parameter has a mixed effect. In principle, its decrease favors the segregation (see above) and increases the surface roughness but decreases the surface mobility and the exchange rate. The actual trend in growth tech-

niques to decrease the growth temperature at very low values ($\approx 300^\circ\text{C}$) by alternating arsenic and third-column atom fluxes (migration-enhanced epitaxy³⁵) leads to an enhancement of the surface mobility of third-column atoms now unimpeded by excess arsenic. No significant reduction of segregation in GaAs/InAs/GaAs structures was obtained by this method.^{4,25} Actually, in the present state of the art in growth techniques, we face contradictory requirements. The number of reaction sites (defects) can be reduced first by stopping the growth at the exact completion of the monolayer—which is possible through the monitoring of RHEED oscillations—and by increasing the surface mobility during the growth of this monolayer. This very mobility will on the other hand enhance the segregation process when the first monolayer of the overlayer is deposited. The logical step could then be to decrease the surface mobility during the growth of the first monolayers of the overlayer, with the risk of obtaining sharp but faulted interfaces.

VII. CONCLUSION

We have reported a systematic study of the segregation to the surface of third-column elements involved in arsenide structures. In all ternary alloys, an important surface enrichment leads to a near-binary surface. In heterojunctions between given binary materials, one of them is abrupt in composition, while the other one is not, due to gradual distribution of the top monolayer of the base material in the growing overlayer. All these behaviors can be summarized by the order for tendency to surface segregation $\text{In} > \text{Ga} \geq \text{Al}$, and by segregation efficiencies which are either near zero or near unity depending on the way structures are built. The interpretation of our data by classical segregation theories yields information about the energetic and kinetic parameters involved. Although the physical origin for the segregation process is not yet clear, these empirical parameters describe correctly the build-up of the composition gradients at heterointerfaces along the growth axis. Our data suggest that these gradients may not be controlled under usual conditions by growth parameters, because of the high segregation energies and fast microscopic phenomena.

ACKNOWLEDGMENTS

We gratefully acknowledge fruitful discussions with J. Y. Marzin, C. A. Sébenne, J. M. Gérard, C. d'Anterrosches, F. Alexandre, M. Quillec, L. Goldstein, F. Mollot, and R. Paniel; acquisition and interpretation of RBS data have been made in collaboration with C. Cohen, F. Abel, D. Schmaus, and A. L'Hoir.

¹The Physics and Technology of Molecular Beam Epitaxy, edited by E. H. Parker (Plenum, New York, 1985).

²B. Deveaux, J. Y. Emery, A. Chomette, B. Lambert, and M. Baudet, Appl. Phys. Lett. **45**, 1078 (1984).

³M. C. Tamargo, R. Hull, L. H. Greene, J. R. Hayes, and A. Y. Cho, Appl. Phys. Lett. **46**, 569 (1985); L. Goldstein, F. Glas, J. Y. Marzin, M. N. Charasse, and G. Le Roux, *ibid.* **47**, 1099 (1985); J. M. Gains, P. M. Petroff, H. Kroemer, R. J. Simes,

- R. S. Geels, and J. H. English, *J. Vac. Sci. Technol. B* **6**, 1378 (1989).
- ⁴J. M. Gérard and J. Y. Marzin, *Appl. Phys. Lett.* **53**, 568 (1988).
- ⁵H. Sakaki, M. Tanaka, and J. Yoshino, *Jpn. J. Appl. Phys.* **24**, L147 (1985).
- ⁶B. Jusserand, E. Alexandre, D. Paquet, and G. Le Roux, *Appl. Phys. Lett.* **47**, 301 (1985); N. Imata, Y. Matsumoto, and T. Baba, *Jpn. J. Appl. Phys.* **24**, L17 (1985); J. C. Lee and T. E. Schlesinger, *J. Vac. Sci. Technol. B* **5**, 1187 (1987).
- ⁷See, for instance, *Grain Boundary Structure and Properties*, edited by G. A. Chadwick and D. A. Smith (Academic, London, 1975); or *Adsorption on Metal Surfaces*, edited by J. Bénard (Elsevier, New York, 1983).
- ⁸T. C. Chiang, R. Ludeke, and D. E. Eastman, *Phys. Rev. B* **25**, 6518 (1982).
- ⁹J. Massies, F. Turco, A. Salettes, and J. P. Contour, *J. Cryst. Growth* **80**, 307 (1987).
- ¹⁰C. Guille, F. Houzay, J. M. Moison, and F. Barthe, *Surf. Sci.* **189/190**, 1041 (1987).
- ¹¹R. A. Stall, J. Zilko, V. S. Swaminathan, and N. Schumaker, *J. Vac. Sci. Technol. B* **3**, 524 (1985).
- ¹²C. Raisin, H. Tegmousse, and L. Lassabatère, *Vide Couches Minces* **41**, 241 (1986).
- ¹³P. C. Zalm, P. M. J. Maree, and R. I. J. Olthof, *Appl. Phys. Lett.* **46**, 597 (1985).
- ¹⁴W. Mönch, R. S. Bauer, H. Gant, and R. Murschall, *J. Vac. Sci. Technol.* **21**, 498 (1982); Ping Chen, D. Bolmont, and C. A. Sébenne, *Surf. Sci.* **132**, 505 (1983).
- ¹⁵T. deJong, W. A. S. Douma, J. F. Van der Veen, F. W. Saris, and J. Haisma, *Appl. Phys. Lett.* **42**, 1037 (1983).
- ¹⁶J. R. Waldrop, R. W. Grant, S. P. Kowalczyk, and E. A. Kraut, *J. Vac. Sci. Technol. A* **3**, 835 (1985).
- ¹⁷D. W. Tu and A. Kahn, *J. Vac. Sci. Technol. A* **3**, 922 (1985).
- ¹⁸K. J. Mackey, P. Allen, W. Herrenden-Harker, and R. H. Williams, *Surf. Sci.* **178**, 124 (1986).
- ¹⁹J. Massies, J. F. Rochette, and P. Delescluse, *J. Vac. Sci. Technol. B* **3**, 613 (1985).
- ²⁰J. M. Moison, C. Guille, M. Van Rompay, F. Barthe, and F. Houzay, *Phys. Rev. B* **39**, 1772 (1989).
- ²¹Ping Chen, D. Bolmont, and C. A. Sébenne, *J. Phys. C* **15**, 6101 (1982); C. R. Brundle, *Surf. Sci.* **48**, 99 (1975).
- ²²J. M. Moison, M. Bensoussan, and F. Houzay, *Phys. Rev. B* **34**, 2018 (1986).
- ²³J. Hornstra and W. J. Bartels, *J. Cryst. Growth* **44**, 513 (1978).
- ²⁴F. Abel, C. Cohen, C. Guille, F. Houzay, A. l'Hoir, J. M. Moison, and D. Schmaus (unpublished).
- ²⁵J. M. Gérard and J. Y. Marzin (private communication).
- ²⁶C. d'Anterrosches, J. M. Gerard, and J. Y. Marzin (unpublished).
- ²⁷M. N. Charasse, Thesis, Université Pierre et Marie Curie, Paris, 1985.
- ²⁸R. Bruisma and A. Zangwill, *Europhys. Lett.* **4**, 729 (1987).
- ²⁹M. DelGuidice, M. Grioni, J. J. Joyce, M. W. Ruckman, S. A. Chambers, and J. H. Weaver, *Surf. Sci.* **168**, 309 (1986); F. Houzay, M. Bensoussan, and F. Barthe, *ibid.* **168**, 347 (1986); Zhangda Lin, F. Xu, and J. H. Weaver, *Phys. Rev. B* **36**, 5777 (1987).
- ³⁰L. J. Brillson, C. F. Bruckner, N. J. Stoffel, A. D. Katnami, and G. Margaritondo, *Appl. Phys. Lett.* **46**, 838 (1982).
- ³¹A. Rosato, K. J. Strandburg, F. Prinz, and R. H. Swendsen, *Phys. Rev. Lett.* **58**, 1038 (1987).
- ³²Y. Gauthier, Y. Joly, R. Baudoin, and J. Rundgren, *Phys. Rev. B* **31**, 6216 (1985); G. Trégliat and B. Legrand, *ibid.* **35**, 4338 (1987).
- ³³C. A. Sébenne, in *Metallization and Metal-Semiconductor Interfaces*, NATO Workshop Proceedings, edited by I. D. Batra (Plenum, New York, 1989).
- ³⁴R. Ludeke, *Surf. Sci.* **132**, 143 (1983).
- ³⁵Y. Horikoshi, M. Kawashima, and H. Yamagushi, *Jpn. J. Appl. Phys.* **25**, L868 (1986).